Journal of Applied Physics

Interplay between quantum paraelectricity and thermoelectricity in the photo-Seebeck effect in a $SrTiO_3$ single crystal

Cite as: J. Appl. Phys. **126**, 045111 (2019); https://doi.org/10.1063/1.5106384
Submitted: 27 April 2019 . Accepted: 05 July 2019 . Published Online: 29 July 2019

Yuuka Shiraishi, Kenji Tanabe, Hiroki Taniguchi, Ryuji Okazaki, and Ichiro Terasaki

COLLECTIONS

Paper published as part of the special topic on Advanced Thermoelectrics
Note: This paper is part of the special topic on Advanced Thermoelectrics.

This paper was selected as Featured

View Online Export Citation CrossMark

ARTICLES YOU MAY BE INTERESTED IN

Room temperature semiconductor detectors for nuclear security
Journal of Applied Physics **126**, 040902 (2019); https://doi.org/10.1063/1.5091805

Applying Tersoff-potential and bond-softening models in a molecular dynamics study of femtosecond laser processing
Journal of Applied Physics **126**, 045109 (2019); https://doi.org/10.1063/1.5096013

Superconducting optoelectronic loop neurons
Journal of Applied Physics **126**, 044902 (2019); https://doi.org/10.1063/1.5096403

Lock-in Amplifiers
... and more, from DC to 600 MHz
Watch

AIP Publishing

© 2019 Author(s).

Journal of Applied Physics ARTICLE scitation.org/journal/jap

Interplay between quantum paraelectricity and thermoelectricity in the photo-Seebeck effect in a $SrTiO_3$ single crystal

Cite as: J. Appl. Phys. **126**, 045111 (2019); doi: 10.1063/1.5106384
Submitted: 27 April 2019 · Accepted: 5 July 2019 ·
Published Online: 29 July 2019

View Online Export Citation CrossMark

Yuuka Shiraishi,[1] Kenji Tanabe,[2] Hiroki Taniguchi,[1] Ryuji Okazaki,[3] and Ichiro Terasaki[1,a)]

AFFILIATIONS

[1]Department of Physics, Nagoya University, Nagoya 464-8602, Japan
[2]Toyota Technological Institute, Nagoya 468-8511, Japan
[3]Department of Physics, Faculty of Science and Technology, Tokyo University of Science, Noda 278-8510, Japan

Note: This paper is part of the special topic on Advanced Thermoelectrics.
[a)]**Email:** terra@nagoya-u.jp

ABSTRACT

We report the electrical conductivity and the Seebeck coefficient of a $SrTiO_3$ single crystal under 405-nm laser illumination from 10 to 30 K. We find that the photoconductivity exponentially increases with decreasing temperature, suggesting a gradual metal-insulator transition. Assuming the carrier mobility reported in the preceding studies, we have evaluated the carrier concentration to be $8 \times 10^9\ cm^{-3}$ at maximum, which corresponds to 10^{-7} ppm impurities in the case of chemical doping. Such ultralow doping is realized only when the energy of the incident light is slightly lower than the bandgap. In this situation, the incident light penetrates the whole sample with a small probability of electron–hole creation. We find that the observed photo-Seebeck coefficient seriously disagrees with the calculated values from the carrier concentration. In order to remedy this discrepancy, we have proposed a phenomenological model in which the quantum paraelectric behavior of $SrTiO_3$ screens the thermoelectric voltage.

Published under license by AIP Publishing. https://doi.org/10.1063/1.5106384

I. INTRODUCTION

When a photon is absorbed in a solid, it generates an electron–hole pair. If the photon energy is higher than the bandgap of a semiconductor, the generated electron and hole can carry electricity by traveling in the conduction and valence bands of the semiconductor. This phenomenon is known as the phototransport and has long been studied for both fundamental and technological points of view. A prototypical example is the photoconductivity that describes an additional contribution to the electrical conductivity induced by light illumination. Another example is the photo-Seebeck effect—the Seebeck effect shown by the photo-induced carriers. Tauc[1] first observed the photo-Seebeck effect in a Ge single crystal in 1955. Since then, this effect has been investigated in several semiconductors as a fundamental probe for carrier dynamics.[2–5] We have studied this effect in wide-gap semiconductors as a novel route for thermoelectric energy conversion[6,7] and measured the photo-Seebeck coefficient in ZnO,[8,9] PbO,[10] Pb_2CrO_5,[11] and ZnS.[12]

To gain a deeper insight into the phototransport phenomena in wide-gap oxides, we focus on the perovskite titanium oxide $SrTiO_3$.[13] This oxide is known as a good photoconductive material, in which the photoconductivity[14,15] and the photo-Hall coefficient[16–18] have been reported at low temperatures. It has also been known as a quantum paraelectric material, and Ishikawa *et al.*[17] have suggested a close relationship between the quantum paraelectricity and the high mobility of the photo-induced electrons. Furthermore, it has been known as one of the promising n-type thermoelectric oxides. Okuda *et al.*[19] reported a large thermoelectric power factor in La-doped $SrTiO_3$ single crystals. Ohta *et al.*[20] evaluated the thermoelectric figure of merit to be around 0.37 at 1000 K in thin-film samples of Nb-doped $SrTiO_3$.

Considering the above features, one can expect a large photo-Seebeck effect in this oxide. Here, we report the photoconductivity and photo-Seebeck coefficient in a $SrTiO_3$ single crystal under 405-nm laser illumination below 30 K. We have observed the

Published under license by AIP Publishing.

photoconductivity of 10^{-6} S/cm and the photo-Seebeck coefficient of -1 to -2 mV/K around 30 K. The carrier concentration calculated from the electrical conductivity is less than 10^{10} cm^{-3}, which is too small to be realized by chemical doping. We find that the measured photo-Seebeck coefficient around 10 K is far smaller in magnitude than the calculation based on the carrier concentration evaluated from the photoconductivity. We propose that the quantum paraelectricity of $SrTiO_3$ screens the thermoelectric voltage induced by photo-doped carriers.

II. EXPERIMENTAL

A $SrTiO_3$ single crystal was purchased from Crystal Base Co., Ltd. The crystal was shaped into a rectangle of $3.6 \times 0.63 \times 0.070$ mm^3, and the indium electrodes were soldered for ohmic contacts. The electrical conductivity and the Seebeck coefficient were measured with two-probe technique under illumination with a home-made measurement station constructed in Physical Property Measurement System (PPMS), Quantum Design. A photographic image of the sample mount is shown in Fig. 1(a), which is constructed on the surface of the rotator sample board in the multifunction probe of PPMS. Figure 1(b) shows a schematic of the sample mount. The high-temperature-side heat bath was made from a sapphire plate pasted on the epoxy sheet equipped with a resistance heater, while the low-temperature side was made from another sapphire plate pasted on copper block. The sample bridged the two plates with varnish, the temperature difference was monitored by a copper-constantan differential thermocouple attached with ultrasonic soldering of indium, and the electrical voltage was measured with the electrodes attached at the edges of the sample.

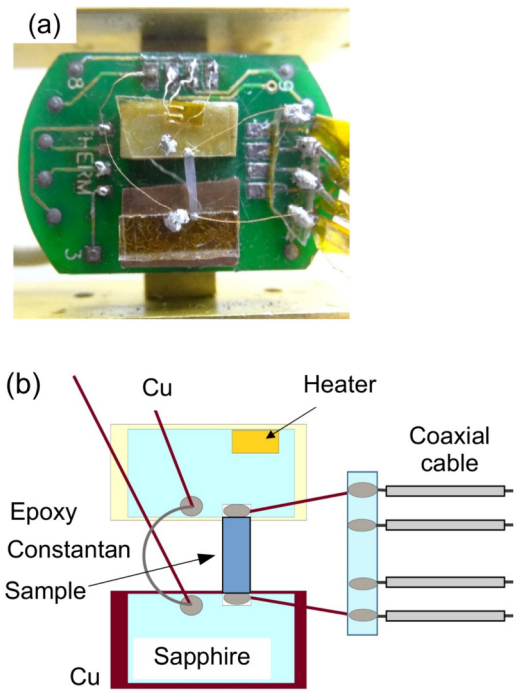

FIG. 1. (a) Photograph of the sample mount. (b) Schematic figure of the sample mount.

We used a 405-nm laser light source guided through an optical fiber on top of the sample, whose photon energy ($\hbar\omega = 3.06$ eV) was slightly lower than the bandgap energy of $SrTiO_3$ ($E_g = 3.25$ eV).[21] In this condition, the incident light is barely absorbed, and consequently, the skin depth of the incident light reaches 5 cm at 295 K,[22] which is much longer than the sample thickness. Thus, the photo-induced carries are generated in the whole sample, and we regard the observed phototransport phenomena as bulk properties.

In our previous studies,[8–12] we used a phenomenological two-layer model including a skin depth as an adjustable parameter on which some of the obtained quantities critically depended. Here, we can analyze the measured value without the two-layer model, which is a big advantage for $\hbar\omega < E_g$. The excitation light intensity ($P_{405\,\mathrm{nm}}$) was 0.1 mW/cm^2 for 100% output, which was weak enough to ignore the temperature rise due to light absorption.

Figure 2 shows a typical measurement sequence for the photo-Seebeck effect. We turn on and off the heater current with a period of 600 s (on for 300 s and off for 300 s) and increases the heater current sequentially. As shown in Fig. 2(b), the temperature difference ΔT monitored by the differential thermocouple shows a square-wave like change and increases from around 0.5 to 1.5 K. The values of ΔT slightly depend on the light intensity, perhaps because the light absorption worked as another heat source that changes the heat flow in the sample. The thermoelectric signal ΔV is shown in Fig. 2(a), and concomitant changes are clearly observed in addition to the substantial noise due to the high resistance of the sample. We notice that the sample temperature changed with the heater current and the light illumination, but the base-temperature change was ± 0.5 K [Fig. 2(c)], which unlikely affected the accuracy of the measurement. Actually, the temperature slope of the Seebeck coefficient was around 0.1 mV/K^2 from 10 to 30 K for $P_{405\,\mathrm{nm}} = 100\%$ [see Fig. 4(b)]. If the base temperature changed by 0.5 K, the Seebeck coefficient might change by 0.05 mV/K. This is too small to explain the huge change of the Seebeck coefficient with $P_{405\,\mathrm{nm}}$ at 25 K in Fig. 4(b).

The photo-Seebeck effect is a change in the Seebeck coefficient with light illumination, which can be observed in principle by subtracting the thermoelectric voltage before and after illumination. However, the light illumination induces photovoltaic voltage at the interface of the electrical contacts, increases the sample temperature, and modifies the temperature difference. Quantitatively, the thermoelectric voltage V_{TE} can be expressed by temperature difference ΔT in the dark as

$$V_{\mathrm{TE}} = S_{\mathrm{dark}}\Delta T + V_0, \tag{1}$$

where S_{dark} is the Seebeck coefficient in the dark and V_0 is the offset voltage. When illuminated, the voltage can be written as

$$V_{\mathrm{TE}} = (S_{\mathrm{dark}} + \delta S)(\Delta T + \delta T) + (V_0 + \delta V_0), \tag{2}$$

where δS is the photo-induced change in the Seebeck coefficient and $S = S_{\mathrm{dark}} + \delta S$ is the photo-Seebeck coefficient. δT and δV_0

Published under license by AIP Publishing.

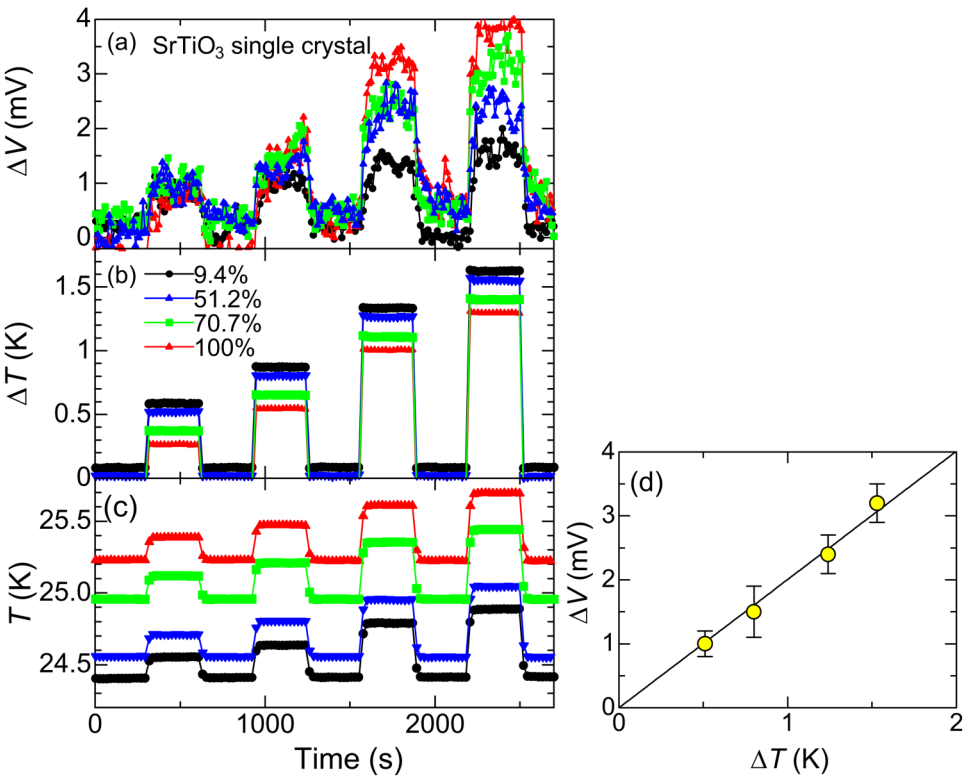

FIG. 2. The photothermoelectric signal plotted as a function of time. The heater current is applied with a time width of 300 s, and the magnitude increases sequentially. (a) Thermoelectric voltage, (b) temperature difference, and (c) sample temperature. The percentages indicated in the figure represent the excitation light intensity ($P_{405\,nm}$), where 100% output corresponds to 0.1 mW/cm^2. (d) The thermoelectric voltage difference ΔV plotted as a function of the temperature difference ΔT for $P_{405\,nm} = 100\%$. The solid line is a linear fitting, from the slope of which the Seebeck coefficient was determined.

are the photo-induced temperature difference and photovoltaic component, respectively. Note that we measured the voltage in a cryostat (Quantum Design PPMS), where the sample temperature was strictly controlled. Then, the photo-Seebeck coefficient is obtained from the slope of V_{TE} against $\Delta T + \delta T$. In the present case, ΔV_{TE}, we found $\Delta V = \Delta V_{TE} = S(\Delta T + \delta T)$, and the photo-Seebeck coefficient S is obtained as $\Delta V/\Delta T$. The sign was carefully determined by the applied polarity. In Fig. 2(d), we show ΔV plotted as a function of ΔT for $P_{405\,nm} = 100\%$ as an example. Linearity was observed within accuracy of 10%, and accordingly, the slope of the fitting line gives S within an accuracy of 10%.

III. RESULTS AND DISCUSSION

We first show the temperature variation of the electrical conductivity measured with several light intensities. The electrical conductivity in the dark was too low to be measured (lower than 10^{-13} S/cm). The electrical conductivity under illumination comes to the measurable range in our setup and shows 8×10^{-6} S/cm at maximum. This means that the photo-induced carriers are successfully doped, and the conductivity has increased more than seven orders of magnitude.

Figure 3 shows the resistance of the single-crystal sample of $SrTiO_3$ plotted as a function of temperature under various light intensities. One can see three remarkable features. The first one is that the low-temperature resistance systematically decreases with increasing light intensity. This indicates that the carriers are doped by photoirradiation. Secondly, the resistance shows a large temperature hysteresis above around 30 K. This hysteresis may be related to persistent photo-doping, although we do not understand the microscopic origin for this. For the third feature, all the resistance curves show anomalous peak just below the cubic-tetragonal transition of 100 K. We do not understand why and how the peak grows around that temperature but find that the metallic conduction appears below the peak. Hereafter, we will focus on the reversible photoconduction below 30 K.

As shown in Fig. 4(a), the electrical conductivity increases exponentially with decreasing temperature. This is in stark contrast with the conductivity of a slightly doped semiconductor, but rather can be regarded as a gradual metal-insulator transition in which dielectric screening due to the quantum paraelectricity of $SrTiO_3$ grows with decreasing temperature. In a doped semiconductor, the ground state change from insulator to metal when the carrier-carrier distance becomes comparable to the spacial dimension of the wave function of a carrier. The latter is characterized by $\varepsilon_r a_B$, where ε_r is the relative dielectric constant and a_B is the Bohr radius. Since ε_r of $SrTiO_3$ rapidly increases below 100 K owing to the quantum paraelectricity, $\varepsilon_r a_B$ increases rapidly at low temperature to stabilize a metallic state with lowering temperature.

Second, we show the temperature dependence of the Seebeck coefficient S measured with several light intensities in Fig. 4(b). The negative sign of the Seebeck coefficient indicates electron-type conduction, consistent with the previous Hall measurement.[16–18] However, we find that the temperature and light-intensity

Published under license by AIP Publishing.

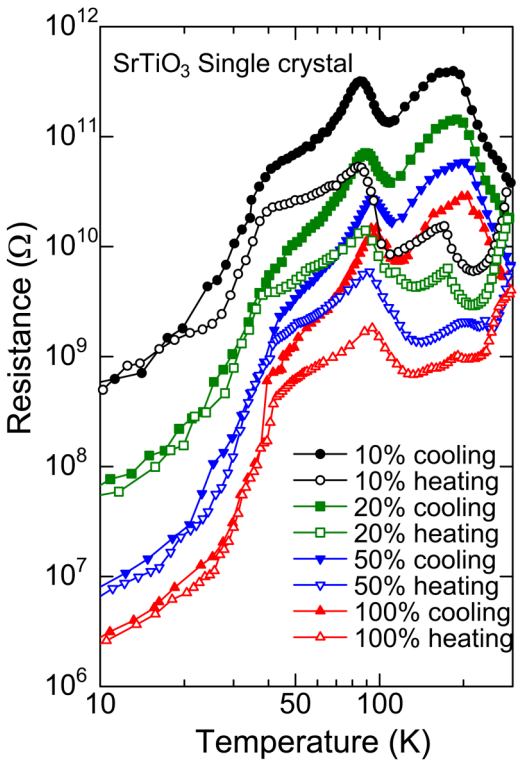

FIG. 3. Resistance of a single-crystal sample of $SrTiO_3$ plotted as a function of temperature with various light intensities. The percentages indicated in the figure correspond to the light intensity of the 405-nm laser light.

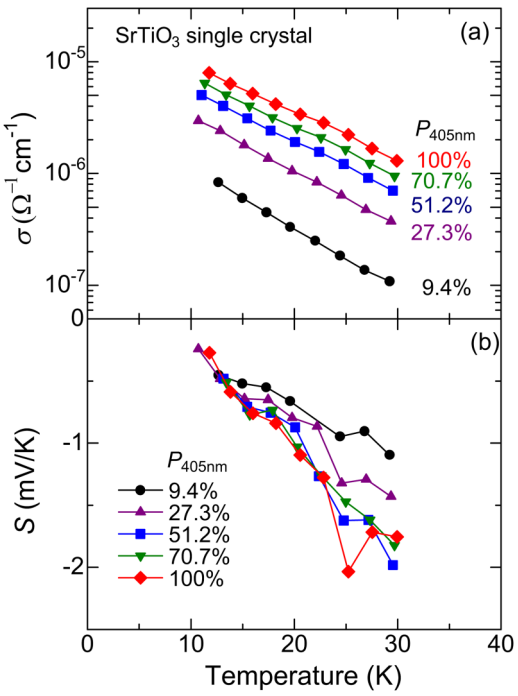

FIG. 4. (a) The electrical conductivity σ as a function of temperature T in a $SrTiO_3$ single crystal measured under the 405-nm laser light with several values of the relative photon flux. (b) The temperature dependence of the Seebeck coefficient S in the same sample under the 405-nm laser light.

dependence deviates from what we expect in a slightly doped semiconductor. $|S|$ decreases rapidly with decreasing temperature and reaches a small value of $250\,\mu V/K$ at 10 K, as if S approached zero toward 0 K. Moreover, $|S|$ "increases" with increasing light intensity. If the light illumination increased electron concentration, it would reduce $|S|$. To be more precise, the Seebeck coefficient for the nondegenerate n-type semiconductor is given by[23]

$$S = -\frac{k_B}{e}\left[\left(r+\frac{5}{2}\right) - \ln\frac{n}{N_c}\right]. \tag{3}$$

Here, n is the carrier concentration and r is the scattering parameter that is defined by the exponent of the energy (ε) dependence of the scattering time $\tau \propto \varepsilon^r$. N_c is the effective density of states given by

$$N_c = 2\left(\frac{2\pi m^* k_B T}{\hbar^2}\right)^{3/2}, \tag{4}$$

where m^* is the effective mass. From Eq. (3), one can see that $|S|$ is a decreasing function of n. Consequently, the light-intensity dependence of $|S|$ seems to be inconsistent with the previous photo-Hall measurement,[18] in which n is found to increase systematically with light intensity.

Let us discuss more quantitatively the photo-Seebeck effect by comparing with the previous reports. The photo-Hall effect in $SrTiO_3$ single crystal reported so far[16–18] indicates that the photo-Hall mobilities are almost independent of photon energies and intensities. Accordingly, we employ the photo-Hall mobility μ_H reported in Ref. 18 and calculate the photo-induced carrier concentration through $n = \sigma/e\mu_H$, where σ is the measured electrical conductivity shown in Fig. 4(a). In Fig. 5(a), we show, thus, obtained n under the 405-nm laser illumination for 100% and 9.4%. n ranges from 10^8 to $10^9\,cm^{-3}$, which corresponds to an impurity concentration of $10^{-8} - 10^{-7}$ ppm. Thus, chemical doping cannot realize such an ultralow value of n, but rather a low rate of electron–hole pair creation caused by the condition of $\hbar\omega < E_g$ can control n down to $10^8\,cm^{-3}$. We emphasize that such an ultralow doping highlights an advantage for carrier-concentration control using photons.

Now we compare S with the calculated value S_{calc} from Eq. (3). We use the above-evaluated n and assume the electron-phonon scattering for $r = -1/2$ and the bare mass for m^*. In Fig. 5(b), we show the calculated values by the dotted curves, which seriously deviate from the measured Seebeck coefficient S_{meas}, as was already discussed qualitatively. In particular, the calculated value S_{calc} weakly depends on temperature, being highly incompatible with S_{meas}.

Published under license by AIP Publishing.

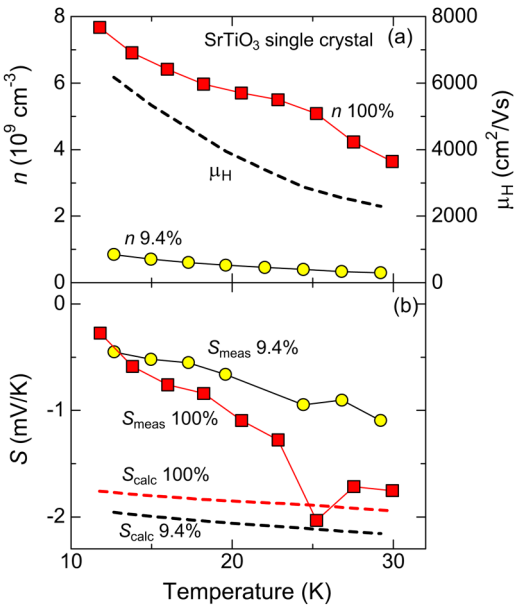

FIG. 5. (a) The temperature dependence of the carrier concentration n in the $SrTiO_3$ single crystal, evaluated from the measured electrical conductivity in Fig. 4(a). The percentages denote the light intensity for 405-nm laser. The data of the photo-Hall mobility μ_H are taken from Ref. 18 as shown by the dotted curve. (b) The measured (S_{meas}) and calculated (S_{calc}) values of the Seebeck coefficient. The percentages denote the light intensity for 405-nm laser.

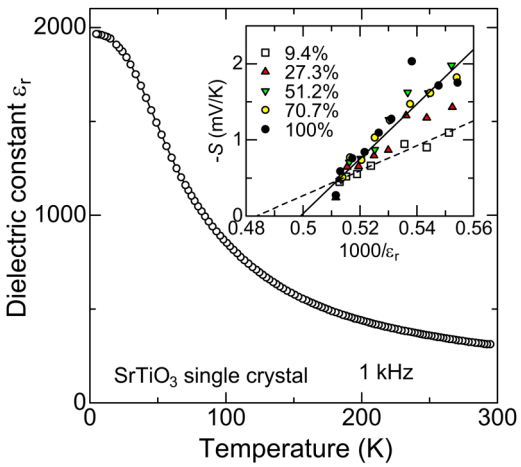

FIG. 6. Dielectric constant of the single-crystal sample of $SrTiO_3$ plotted as a function of temperature. The inset shows the photo-Seebeck coefficient plotted as a function of inverse dielectric constant $1000/\varepsilon_r$.

Here, we briefly discuss a possible contribution from phonon drag. Okuda *et al.*[19] found a phonon-drag term in a sample with a carrier concentration of $10^{20}\,cm^{-3}$, but the magnitude was around 0.25 mV/K at 50 K at maximum, being one order of magnitude smaller than S_{meas}. Also, the sign was negative, namely, the Seebeck coefficient was enhanced by phonon drag, which is opposite situation of $|S_{meas}| < |S_{calc}|$. Since electrons should be degenerate to show the drag effect, the phonon-drag term may be present at much lower temperatures with much smaller magnitude. Thus, we can ignore the phonon-drag effect in the present experiment.

One possible origin of this discrepancy arises from the screening effects by the depolarization field. $SrTiO_3$ is known as a quantum paraelectric material,[13] which shows an increasingly huge permittivity with decreasing temperature. Moreover, the generated carrier density of $10^9\,cm^{-3}$ is too small to screen the internal electric field. In these conditions, the thermoelectric field arising from the temperature gradient induces the polarization that generates the electric field along the opposite direction to the thermoelectric field. Let us discuss this situation with a classical electromagnetism. The polarization $\boldsymbol{P}$ and the electric field $\boldsymbol{E}$ satisfy

$$\boldsymbol{P} = \varepsilon_0\chi_e\boldsymbol{E} = \varepsilon_0\chi_e(\boldsymbol{E}_c + \boldsymbol{E}_{th}), \tag{5}$$

where ε_0 is the dielectric constant of vacuum and χ_e is the electric susceptibility. $\boldsymbol{E}$ is further written as a sum of the depolarization field $\boldsymbol{E}_c$ and the thermoelectric field $\boldsymbol{E}_{th}$. $\boldsymbol{E}_c$ is associated with the depolarization factor N_d as

$$\boldsymbol{E}_c = -\frac{N_d\boldsymbol{P}}{\varepsilon_0}. \tag{6}$$

By eliminating $\boldsymbol{P}$ from Eqs. (5) and (6), we get

$$\boldsymbol{E}_c = -\frac{N_d\chi_e}{1+N_d\chi_e}\boldsymbol{E}_{th}. \tag{7}$$

The measured Seebeck coefficient is given by definition as

$$S_{meas} = \frac{E}{dT/dx} = \frac{1}{1+N_d\chi_e}\frac{E_{th}}{dT/dx}. \tag{8}$$

This equation tells us that $E_{th} \sim S_{calc}dT/dx$ is reduced by the large electric susceptibility χ_e of $SrTiO_3$. If we assume $N_d = 1/3$ for the sake of simplicity, we arrive at $S_{meas} \propto 1/\varepsilon_r$ for $\chi_e \gg 1$, where ε_r is the relative dielectric constant.

In Fig. 6, the relative dielectric constant ε_r of the same sample is shown as a function of temperature at 1 kHz. Reflecting the quantum paraelectricity, the dielectric constant rapidly grows with decreasing temperature and tends to saturate below 20 K. In the inset, we compare the measured $1000/\varepsilon_r$ and the photo-Seebeck coefficient S. One can find that all the data are linear in $1000/\varepsilon_r$.

However, S is not proportional to $1/\varepsilon_r$. The dotted and solid lines are guides to the eye for 9.4% and 100% illumination and cross the x axis at 0.48 and 0.50, respectively. This means that thermoelectric voltage is screened, when ε_r reaches a certain value around 2000.

Published under license by AIP Publishing.

IV. SUMMARY

In summary, we have measured the temperature dependence of the electrical conductivity and the Seebeck coefficient in a $SrTiO_3$ single crystal under the 405-nm laser illumination. The conductivity increases exponentially with decreasing temperature, making a remarkable contrast to the conventional doped semiconductors. We have calculated the carrier concentration from the measured conductivity and find that the carrier concentration ranges from 10^8 to 10^9 cm^{-3}. Such an ultralow doping is only possible in the photo-doping with a photon energy slightly lower than the bandgap. The ultralow doped $SrTiO_3$ shows strong depolarization effects arising from the quantum paraelectric behavior at low temperatures and exhibits a significantly reduced Seebeck coefficient. In this respect, the quantum paraelectricity is detrimental to photothermoelectrics unfortunately,[6] but instead it induces an unconventional metallic state to be explored, in which the conductivity exponentially increases with decreasing temperature. The technique developed in the present paper has revealed how the charge transport evolves below the critical carrier concentration for the metal-insulator transition.

ACKNOWLEDGMENTS

This work was partially supported by ALCA, Japan Science and Technology Agency, Japan and by Grant-in-Aid for Scientific Research, Japan Society for the Promotion of Science, Japan (Kakenhi No. 26287064). This work was performed under the Cooperative Research Program of "Network Joint Research Center for Materials and Devices." We also wish to thank Y. Yasui, M. Fujita, and H. Ohta for close collaboration of this work.

REFERENCES

[1]J. Tauc, Czech. Phys. J. **5**, 528 (1955).
[2]R. Lawrance and R. H. Bube, J. Appl. Phys. **39**, 1807 (1968).
[3]J. G. Harper, H. E. Matthews, and R. H. Bube, J. Appl. Phys. **41**, 3182 (1970).
[4]J. G. Harper, H. E. Matthews, and R. H. Bube, J. Appl. Phys. **41**, 765 (1970).
[5]H. B. Kwok and R. H. Bube, J. Appl. Phys. **44**, 138 (1973).
[6]I. Terasaki, R. Okazaki, P. S. Mondal, and Y.-C. Hsieh, Mater. Renew. Sustain. Energy **3**, 29 (2014).
[7]I. Terasaki, R. Okazaki, and H. Ohta, Scr. Mater. **111**, 23 (2016).
[8]R. Okazaki, A. Horikawa, Y. Yasui, and I. Terasaki, J. Phys. Soc. Jpn. **81**, 114722 (2012).
[9]A. Horikawa, T. Igarashi, I. Terasaki, and R. Okazaki, J. Appl. Phys. **118**, 095101 (2015).
[10]P. S. Mondal, R. Okazaki, H. Taniguchi, and I. Terasaki, J. Appl. Phys. **114**, 173710 (2013).
[11]P. S. Mondal, R. Okazaki, H. Taniguchi, and I. Terasaki, J. Appl. Phys. **116**, 193706 (2014).
[12]Y. Shiraishi, R. Okazaki, H. Taniguchi, and I. Terasaki, Jpn. J. Appl. Phys. **54**, 031203 (2015).
[13]T. Sakudo and H. Unoki, Phys. Rev. Lett. **26**, 851 (1971).
[14]H. Katsu, H. Tanaka, and T. Kawai, Jpn. J. Appl. Phys. **39**, 2657 (2000).
[15]K. X. Jin, B. C. Luo, Y. F. Li, C. L. Chen, and T. Wu, J. Appl. Phys. **114**, 033509 (2013).
[16]H. Yasunaga, J. Phys. Soc. Jpn. **24**, 1035 (1968).
[17]T. Ishikawa, M. Kurita, H. Shimoda, Y. Sakano, S.-Y. Koshihara, M. Itoh, and M. Takesada, J. Phys. Soc. Jpn. **73**, 1635 (2004).
[18]Y. Kozuka, Y. Hikita, T. Susaki, and H. Y. Hwang, Phys. Rev. B **76**, 085129 (2007).
[19]T. Okuda, K. Nakanishi, S. Miyasaka, and Y. Tokura, Phys. Rev. B **63**, 113104 (2001).
[20]S. Ohta, T. Nomura, H. Ohta, M. Hirano, H. Hosono, and K. Koumoto, Appl. Phys. Lett. **87**, 092108 (2005).
[21]K. van Benthem, C. Elsässer, and R. H. French, J. Appl. Phys. **90**, 6156 (2001).
[22]M. Capizzi and A. Frova, Phys. Rev. Lett. **25**, 1298 (1970).
[23]G. D. Mahan, Solid State Phys. **51**, 81 (1998).

Published under license by AIP Publishing.